Cytometry
PART A
Journal of the International Society for Advancement of Cytometry

MIFlowCyt

Use of LysoTracker Dyes: A Flow Cytometric Study of Autophagy

Shaheen Chikte, Neelam Panchal, Gary Warnes*

Flow Cytometry Core Facility, The Blizard Institute, Barts and The London School of Medicine and Dentistry, London University, London, E1 2AT, United Kingdom

Additional Supporting Information may be found in the online version of this article.

Correspondence to: Gary Warnes, The Flow Cytometry Core Facility, The Blizard Institute, Barts and London School of Medicine and Dentistry, London University, 4 Newark Street, London E1 2AT, United Kingdom.
E-mail: g.warnes@qmul.ac.uk

Published online 11 July 2013 in Wiley Online Library (wileyonlinelibrary.com)

DOI: 10.1002/cyto.22312

- The flow cytometric use of LysoTracker dyes was employed to investigate the autophagic process and to compare this with the upregulation of autophagy marker, the microtubule-associated protein LC3B. Although the mechanism of action of LysoTracker dyes is not fully understood, they have been used in microscopy to image acidic spherical organelles, and their use in flow cytometry has not been thoroughly investigated in the study of autophagy. This investigation uses numerous autophagy-inducing agents including chloroquine (CQ), rapamycin, low serum (<1%) RPMI, and nutrient starvation to induce autophagy in Jurkat T-cell leukemia and K562 erythromyeloid cell lines. LC3B showed an increase with CQ treatment although this was different to LysoTracker signals in terms of dose and time. Rapamycin, low serum (<1%) RPMI, and nutrient starvation induction of autophagy also induced an increase in LysoTracker and LC3B signals. CQ also induced apoptosis in cell lines, which was blocked by pan-caspase inhibitor z-VAD resulting in a reduction in cells undergoing apoptosis and a subsequent upregulation of autophagic markers LC3B and lysosomal dye signals. Given that LC3B and LysoTracker are measuring different biological events in the autophagic process, they surprisingly both upregulated during autophagic process. This study, however, shows that although LysoTracker dyes do not specifically label lysosomes or autophagosomes within the cell, they allow the simultaneous measurement of an autophagy-related process and other live-cell functions, which are not possible with the standard LC3B antibody-labeling technique. This method has the advantage of other live-cell LCB-GFP-tagged experiments in that be used to analyze patient cells as well as easier to use and significantly less costly.
© 2013 International Society for Advancement of Cytometry

- **Key terms**
autophagy; LysoTracker; LC3B; annexin V

THE term autophagy (Type II Apoptosis) is derived from the Greek roots "auto" (self) and "phagy" (eat) and was first observed by Porter in 1962 and the term was coined by De Duve in 1967 to epitomize this type of cell death (1,2). Even though it was described 50 years ago, much about this process is yet unknown (3,4). Autophagy describes an intracellular bulk degradation system that channels malfunctioning components into the lysosomal machinery of the cell, and it is unclear whether the process protects or causes diseases such as cancer and neurodegenerative disorders (5,6). Components degraded via autophagy may range from proteins to entire organelles (e.g., mitochondria) to invading microbes and may be targeted specifically or nonspecifically (7–10).

Autophagy is characterized by the formation of a double membrane around the cytostolic components to be degraded, forming an autophagosome (3,11) that then fuses with nearby lysosomes, giving rise to an autolysosome, where the intracellular components are degraded by hydrolytic enzymes (3,4). The process of autophagy is a cell-survival mechanism that occurs when the cell is under stress from external environmental pressures, including the lack of nutrients, or the internal microenvironment of the cell.

Methods for monitoring autophagy started with the initial discovery of the process by the use of electron microscopy showing the presence of double and single

ISAC
International Society for Advancement of Cytometry

membrane structures termed the autophagosome and autolysosome or autophagolysosome, respectively (1,2). Biochemical techniques such as Western blotting can be used to quantitate the degree of autophagy in cells by measuring the autophagy marker protein, microtubule-associated protein light chain LC3I and LC3II (or LC3B as referred to from here on), which is normally located in the cytoplasm in the form of LC3I, but when cleaved and lipidated by phosphotidylethanolamine, is then incorporated into the autophagosome in the form of LC3B (12–14). LC3B can also be imaged and flow cytometrically analyzed with the addition of a fluorescent tag via transfections with GFP, with the benefit that GFP fluorescence is dissipated by the acidic conditions prevailing in autolysosomes, thus making LC3B-GFP detection-specific for autophagosomes (13,15–17). The increase in number and intensity of fluorescently labeled anti-LC3B-positive autophagosomes–autolysosomes can be quantitated by time-consuming image analysis, whereas increase in median fluorescent values of LC3B antigen levels flow cytometrically makes the process significantly less burdensome (16,18–20).

Invitrogen's LysoTracker dyes label-acidic spherical granules within cells and are not lysosome-specific. The mechanism of retention within the granules is not established although its fluorescence is not reversed by weak basic compounds. The use of LysoTracker probes has also been used to investigate the degree of autophagy occurring by the measurement of their fluorescence by microscopy and to a limited extent by flow cytometry (21–25). The new autophagy dye from Enzo, Lyso-ID, has also similarly been used to monitor lysosome mass co-localized with LC3B during the autophagic process by image cytometry (26).

This study compares anti-LC3B-staining levels to LysoTracker Green (LTG) signals measured flow cytometrically and confirmed by fluorescent microscopy using two chemical inducers and inhibitors of autophagy and apoptosis as well as serum and nutrient depravation using Jurkat T-cell leukemia and K562 erythromyeloid leukemia cell lines. CQ not only induces autophagy but also then inhibits the process by blocking lysosomal fusion with the autophagosome by disruption of vesicular acidification, resulting in a build up of autophagosomes and lysosomes within the cell (21,22,27). The employment of various reagents was chosen for specific purposes, in that CQ does not create an autophagic flux and thus generates a large signal that can be more easily detected flow cytometrically. Whilst rapamycin and starvation inhibit the action of a nutrient-responsive serine–threonine kinase mTOR, resulting in cell-cycle arrest, generating an autophagic flux (or throughput of autophagosomes–autolysosomes), and thus, at any one time, the autophagic machinery that can be detected is much lower than displayed by CQ, thus testing the sensitivity of these flow cytometric assays to detect autophagy (28–31). Because CQ also induces apoptosis, but rapamycin does not, modulation of the level of autophagy as detected by flow cytometric measurement of LC3B and LTG signals was investigated by the employment of the pan-caspase blocker z-VAD, which should result in a detectable increase in the autophagic signals produced by CQ but not rapamycin (30).

The autophagic process appears to involve the generation of more lysosomes that fuse with the autophagosome resulting in the formation of the autophagolysosome, thus allowing the flow cytometric quantitation of the autophagic process indirectly in live cells allowing the simultaneous measurement of other cell functions such as mitochondrial function, ER, and mitochondrial autophagy (21,22,27). The use of the Invitrogen LTG dye was used to quantitate indirectly the degree of autophagy in two cell lines, Jurkat T-cells, and the erythromyeloid leukemia cell line, K562. Increase in LysoTracker signal was compared flow cytometrically to the level of LC3B formation as detected by fluorescently tagged antibody in K562 and Jurkat cell lines. This comparison of the acidic granule and LC3B levels (a marker of autophagy) that the LTG dye and anti-LC3B, respectively, measures, is consequently not a direct comparison of the same processes involved in autophagy. The development of a cheap, reproducible, and easy flow cytometric-based method to determine the degree of autophagy in live cells will enhance the ability to study the cell death processes and mechanisms involved in autophagy in primary cells isolated from patients as well as cell lines.

Materials and Methods

Cell Lines

Jurkat T and K562 cell lines were grown in Roswell Park Memorial Institute (RPMI)-1640 with L-glutamine (cat. no. 21875-034, Invitrogen, Paisley, UK) supplemented with 10% fetal bovine serum (cat. no. 10500-064, Invitrogen) and penicillin and streptomycin (cat. no. 15140-122, Invitrogen) in the presence of 5% CO_2 at 37°C.

Induction of Autophagy

Jurkat and K562 cells were treated with chloroquine (CQ) at 25, 50, and 75 μM, (cat. no. C6628-25G, Sigma, Poole, UK) or rapamycin (40 and 80 nM, cat. no. PHZ1233, Invitrogen). Jurkat and K562 cells were also grown in low-serum conditions (<1%) in RMPI-1640 with L-glutamine and low-serum conditions (<1%) in phosphate-buffered saline (PBS; cat. no. 14190-094, Invitrogen). Time points analyzed were 24 and 48 h ($n = 3$) as described in the following section. Cells were also pretreated with z-VAD-FMK at 5 μM (cat. no. V116-2MG, Sigma, Poole, UK) for 1 h in culture before the addition of 50 μM CQ or 80 nM rapamycin.

Lysotracker Labeling

Jurkat and K562 cells with or without treatment were loaded LTG (50 nM, cat. no. L7526, Invitrogen) according to the manufacturer's instructions by incubating cells with dye for 1 h at 37°C, respectively (see Supplementary Information Figure 1). LTG loading was shown to be optimal at 50 nM after 1-h incubation for both cell lines. Cells were then washed in PBS buffer and resuspended in 400 μl of PBS in the presence of DNA viability dye, 4',6-diamidino-2-phenylindole (DAPI; 200 ng/ml; cat. no. D9542, Sigma Chemicals, Poole, UK). Live cells were analyzed for LTG median fluorescence intensity (MFI) levels by first gating on all cell material except small debris in the origin of a FSC versus SSC dot-plot. This data was then analyzed on a DAPI versus FSC dot-plot with

live cells being DAPI−ve. LTG signals from samples were then compared by histogram analysis of MFI. LTG MFI upregulation from autophagy-induced samples and untreated cells were compared to show the average fold increase and the individual data points shown ($n = 3$). About 100,000 events were collected by flow cytometry.

Indirect Immunofluorescence LC3B labeling

Jurkat and K562 cells with or without treatment were pelleted and resuspended in 100 μl of Solution A fixative for 15 min at room temperature (RT; cat. no. GAS-002A-1, Caltag, UK). Cells were then washed in PBS buffer. Cell pellets were then permeabilized with 0.25% Triton X-100 (cat. no. X100–500ML, Sigma Chemicals) for 15 min at RT. Cells were washed in PBS buffer. Anti-LC3B polyclonal antibody (0.25 μg; cat. no. L10382, Invitrogen) or rabbit immunoglobulin (0.25 μg; cat No I5006, Sigma Chemicals) was used as an isotype control and incubated for 0.5 h at RT. Cells were then washed in PBS buffer. Cells were then labeled with 0.125 μg of secondary fluorescent conjugate Alexa Flour 647 goat anti-rabbit IgG (cat. no. A21244, Invitrogen) for 30 min at RT. Cells were then washed in PBS buffer and resuspended in 400 μl of PBS in the presence of DNA viability dye, DAPI (200 ng/ml), see Supplementary Information figure 2. Analysis of LC3B-Alexa Fluor647 signal was achieved by determining the MFI of the whole histogram signal for previously live cells gated from a FSC versus SSC dot-plot. LC3B MFI upregulation from autophagy-induced samples and untreated cells were compared to show the degree of induced autophagy. Average fold increase for autophagic samples was calculated from average control MFI LC3B levels and the individual data points shown ($n = 3$). LC3B-labeled samples were also compared to corresponding isotype control samples in an overlaid histogram. About 10,000 events were collected by flow cytometry.

Annexin V Labeling

Jurkat and K562 cells at 24 and 48-h time points for untreated and treated cells were resuspended in 100-μl calcium-rich buffer (cat. no. 556454, Becton Dickinson, San Jose, CA), with annexin-FITC (2.5 μl; cat. no. 556547, Becton Dickinson). Cells were then incubated at RT for 15 min. DNA viability dyes, DAPI (200 ng/ml), was added just before flow cytometric analysis. Gating of cells was carried out by gating on them via a FSC versus SSC dot-plot excluding very small debris in the origin only. Live (double negative), apoptotic (annexin V+ve/DAPI−ve), and dead cells (annexin V+ve or −ve/DAPI+ve) were then determined in percentages via quadrant analysis of dot-plots of annexin V-FITC versus DAPI dot-plots.

Flow Cytometry

Single-color controls for annexin V-FITC or LTG, DAPI, and unstained cells were used to set compensations. Annexin V-FITC or LTG was detected in the 530/25 nm channel on the argon laser octagon (BD FACSCanto II 286/360v); DAPI was detected in the 440/40 nm channel on the violet diode trigon (BD FACSCanto II 352/324v). LC3B-Alexa Fluor-647-labeled cells and DAPI (200 ng/ml) were analyzed on the 660/20 nm channel on 440/40 nm channel on the red He–Ne and violet diode trigons (BD FACSCanto II 456v/308v).

Cells were analyzed on a Becton Dickinson FACSCanto II fitted with a 488-nm Ti-sapphire argon laser, red He–Ne 633 nm laser, and violet diode 405 nm with FACSDiva Software ver 6.1.3 (Becton Dickinson). All data were analyzed on FlowJo (ver 8.8.7, Treestar, CA) in the form of list-mode data files version FCS 3.00 using the default bi-exponential transformation. Optical filters and mirrors in the BD FACSCanto II were fitted in 2008.

Fluorescent Imaging

Cells labeled with LC3B-Alexa-Fluor-647 or LTG and counter stained with DAPI at 24 and 48 h were pelleted and 10 μl placed on glass microscope slide, mounted with a coverslip, and sealed with nail varnish. Cells were imaged using a Zeiss 510 confocal microscope (Jena, Germany) fitted with a meta-head detection system and argon laser (488 nm), violet diode (405 nm), and red He–Ne (633 nm) laser. LTG was excited with the 488 nm laser and imaged in the 530/30 nm channel; DAPI was excited with the 405 nm laser and imaged in the 440/40 nm channel; anti-LC3B-Alexa Fluor-647 was excited by the red He–Ne (633 nm) laser and imaged in the 660LP channel. Quantification of LC3B-Alexa-Fluor-647 and LTG fluorescence at 660 and 530 nm was determined by the use of GT Vision (GT Vision, Suffolk, UK) image analysis software (Gx capture software Ver.6.2.3.0) by the generation of fluorescence histograms at 660 and 530 nm to determine the level of LC3B and LTG fluorescence. Histograms show increasing fluorescence from left to right (x-axis) and the number of pixels (y-axis).

Statistics

T tests were performed using a two-tailed distribution with two sample unequal variances using Minitab 15 software when comparing treatment samples to untreated controls for K562 and Jurkat cell lines. ANOVA statistical analysis was performed using Minitab 15 software to compare differences with and without z-VAD pretreatment. $P = >0.05$ not significant (NS), $P = <0.05^{*}$, $P = <0.01^{**}$, and confidence limits set at 95% or 0.05.

Results

Comparison of LC3B and LTG Upregulation in the Detection of CQ-Induced Autophagy in Jurkat and K562 Cells

Compounds used to induce an autophagic flux, for example, rapamycin, produce a throughput of autophagic machinery making the signal to detect flow cytometrically small, thus testing the sensitivity of the assay. Conversely, CQ due to its inhibitory action produces a larger autophagic signal that is easier to detect flow cytometrically in a similar manner to that employed by the use of Golgi stop reagents in the flow cytometric detection of intracellular cytokines. The upregulation of autophagy marker LC3B was compared to the increase in LTG signal observed after CQ treatment. Anti-LC3B-AlexaFluor647 labeling showed that untreated K562 cells had detectable amounts of LC3B (Fig. 1A) compared to

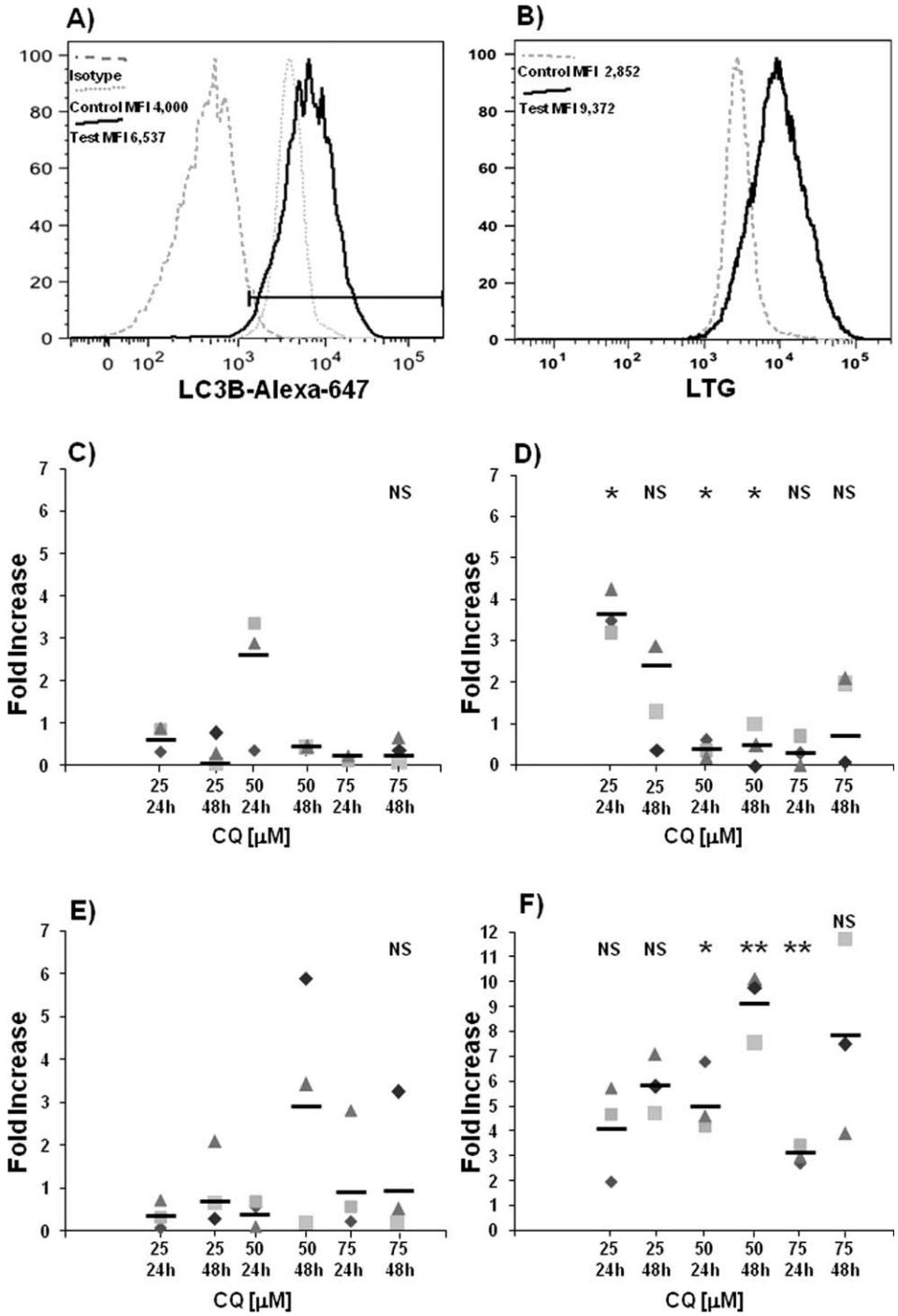

Figure 1. K562 and Jurkat cell lines were untreated or treated with CQ at 25, 50, and 75 μM for 24 and 48 h. Cells were labeled with anti-LC3B-Alexa Fluor647 or isotype-Alexa Fluor647 or 50 nM LTG at 24 and 48 h. Histogram overlays of K562 LC3B expression of isotype control, untreated cells, and cells treated with 50 μM CQ at 24 h are shown in (**A**). Histogram overlays of K562 LTG expression of untreated cells and cells treated with 25 μM CQ at 24 h are shown in (**B**). Median fluorescence intensity (MFI) values are indicated in (A, B). K562 and Jurkat cell LC3B MFI expressions for untreated or 25, 50, and 75 μM CQ were determined flow cytometrically at 24 and 48 h and expressed as fold increase above untreated cell controls (**C**, **E**). K562 and Jurkat cell LTG MFI expression for untreated cells or 25, 50, and 75 μM CQ were determined flow cytometrically at 24 and 48 h and expressed as fold increase above untreated cell controls (**D**, **F**). *T* test, $*P = < 0.05$, $**P = < 0.01$; NS, not significant; black bars indicate average fold increase, and each individual data point are also shown, $n = 3$.

the isotype control and that cells treated with 50 μM CQ showed an upregulation of LC3B above control levels (Fig. 1A). Likewise, LTG showed a threefold upregulation of the LTG signal when K562 cells were treated with 25 μM CQ compared to untreated controls (Fig. 1B). K562 cells gave a dose-dependent induction of autophagy by CQ (25, 50, and 75

μM) with a doubling in LC3B MFI in the case of 50 μM CQ treatment. A lower increase of 30% in LC3B upregulation was observed at 25 μM CQ at 24 h; with virtually no increase observed at 75 μM CQ (10%; Fig. 1C). Similarly, the Jurkat cell LC3B response to CQ showed a dose-dependent induction of autophagy (25, 50, and 75 μM) with a maximum increase of 90% in LC3B MFI, but at 75 μM CQ (Fig. 1E). Lower increases (40%) in LC3B upregulation were observed at 25 and 50 μM, respectively, at 24 h (Fig. 1E). Jurkat cell LC3B upregulatory response to CQ was maintained at 48 h for all concentrations of CQ, maximizing by threefold at 50 μM (Fig. 1E), whilst K562 cells showed minimal upregulation at 48 h (Fig. 1C).

CQ treatment of K562 cells at 50 μM induced optimal LC3B upregulation at 24 h, while these cells gave much higher LTG signals at 25 μM CQ, which showed a two to fourfold increase above control levels at 24 and 48 h, respectively, $P = <0.05$ (Fig. 1D). K562 cells, which, at 48 h, had basal levels of LC3B, showed minimal changes in LTG signal at 48 h compared to that detected at 24 h, $P = <0.05$ (Fig. 1D). Jurkat cells in a similar manner to K562 cells showed increased LTG signals of three to fivefold at 24 h, with a maximum signal at 50 μM CQ, $P = <0.05$ (Fig. 1F). Interestingly, Jurkat cells, like K562, showed a similar maintenance of the LTG response at 48 h, with an increase from six to ninefold above control levels (Fig. 1F).

Comparison of LC3B and LTG Upregulation in the Detection of Rapamycin and Nutrient Starvation-Induced Autophagy in Jurkat and K562 Cells

Rapamycin and nutrient starvation induces autophagy by inhibiting the action of nutrient-responsive kinase, serine–threonine kinase, mTOR. However, unlike CQ, there is no blockade of autophagy and, consequently, no autophagic flux hence only relatively small autophagic signals that can be measured flow cytometrically at any one time. Rapamycin was thus included in this study to demonstrate the sensitivity of the flow cytometric detection of LC3B and LTG. Untreated K562 cells have detectable amounts of LC3B (Fig. 2A) compared to the isotype control, and cells treated with 80 nM rapamycin showed an upregulation of LC3B (Fig. 2A). Likewise, LTG showed an upregulation of the LTG signal when K562 cells are treated with 80 nM rapamycin compared to untreated controls (Fig. 2B).

Induction of autophagy of K562 cells by rapamycin resulted in significantly high signals (three to fivefold increase, respectively) at 24 and 48 h for LC3B, respectively (Fig. 2C). Jurkat cells responded to rapamycin in a similar manner with significantly high signals (six and fourfold increase, respectively) for all drug concentrations at 24 and 48 h for LC3B, respectively (Fig. 2E). Low-serum and nutrient-free conditions induced a significant twofold increase in K562 LC3B levels at both time points (Fig. 2C). In contrast, Jurkat cells showed a much larger LC3B response at 48 h when grown in low-serum conditions, conversely, low-nutrient levels only induced a high level of LC3B at 24 h (Fig. 2E).

K562 cells treated with rapamycin showed an increase (20%) in the detectable LTG signal at 24 h, which returned to basal levels at 48 h (Fig. 2D). Again, Jurkat cells in comparison with K562 cells showed a smaller increase in LTG signals (10%) with rapamycin treatment at 24 h ($P = $ NS) and no signal above control levels at 48 h (Fig. 2F). Similarly, K562 cells in low-serum growth conditions induced only a 20% increase in LTG at 48 h and a small increase (10%) when cells were placed in nutrient-free conditions (Fig. 2D). In contrast, Jurkat cells showed a two to fourfold increase in LTG in response to low-serum conditions with a small increase (30%) observed at 24 h when Jurkat cells were placed in low-nutrient conditions (Fig. 2E).

Imaging of Autophagic LC3B and LTG Upregulation

Resting K562 and Jurkat cells were imaged by confocal microscopy for LC3B levels after labeling with Alexa-647 and counterstaining with DAPI (Fig. 3). CQ and rapamycin-treated K562 and Jurkat cells showed larger LC3B signals than resting cells; this was confirmed visually and by semiquantitative histogram analysis of red fluorescence at 660 nm (Figs. 3A–3F). Resting K562 and Jurkat cells were imaged by confocal microscopy for LTG levels after labeling with LTG and counterstaining with DAPI (see Figs. 3G and 3J). CQ and rapamycin-treated K562 and Jurkat cells showed larger LTG signals than resting cells; this was confirmed visually and by semiquantitative histogram analysis of green fluorescence at 530 nm (Figs. 3G–3L).

zVAD Blockade of Apoptosis to Demonstrate Upregulation of Autophagy Markers

CQ also induces apoptosis, whilst rapamycin does not; thus pretreatment of K562 cells with pan-caspase inhibitor, zVAD before CQ treatment, should result in changes in levels of live cells, annexin V-binding cells, and dead cells induced by CQ alone (Fig. 4). Pretreatment of K562 cells with z-VAD and then CQ showed a larger significant rescue of cells from apoptosis ($P < 0.05$) than observed with Jurkat cells, because the level of cell death was much greater in the Jurkat cell response to CQ compared to K562 (Figs. 4A–4H). This was in contrast to zVAD-rapamycin treatment, which showed minimal changes in signals for both cell lines (data not shown).

Likewise, ideally, the autophagic LC3B and LTG signal in z-VAD-CQ-treated cells should increase above that detected by CQ alone, given that the cells are all then been channeled through the autophagic route of cell death (Fig. 5). This was observed with K562 LC3B expression, presented in an overlay of control cells, 50 μM CQ, and z-VAD+50 μM CQ with an average fivefold increase at 48 h (Figs. 5A and 5C). In contrast, the forecast increase in LTG signal resultant from a build up of lysosomes occurred at 24 h not 48 h, with K562 cells giving a threefold increase in LTG signal with z-VAD-CQ treatment compared to CQ treatment alone at 24 h (Figs. 5B and 5D). In contrast, Jurkat cells only showed a 50% increase in LC3B signal, with no change in LTG signal was observed after z-VAD pretreatment at 24 h, respectively (Figs. 5E and 5F). At 48 h, the Jurkat autophagic signals measured by LTG and LC3B increased by two and threefold above CQ treatment alone, respectively (Figs. 5E and 5F). The z-VAD pretreatment with 80 nM rapamycin on both cell lines showed no significant difference to 80 nM rapamycin treatment alone at 24 and 48 h (data not shown).

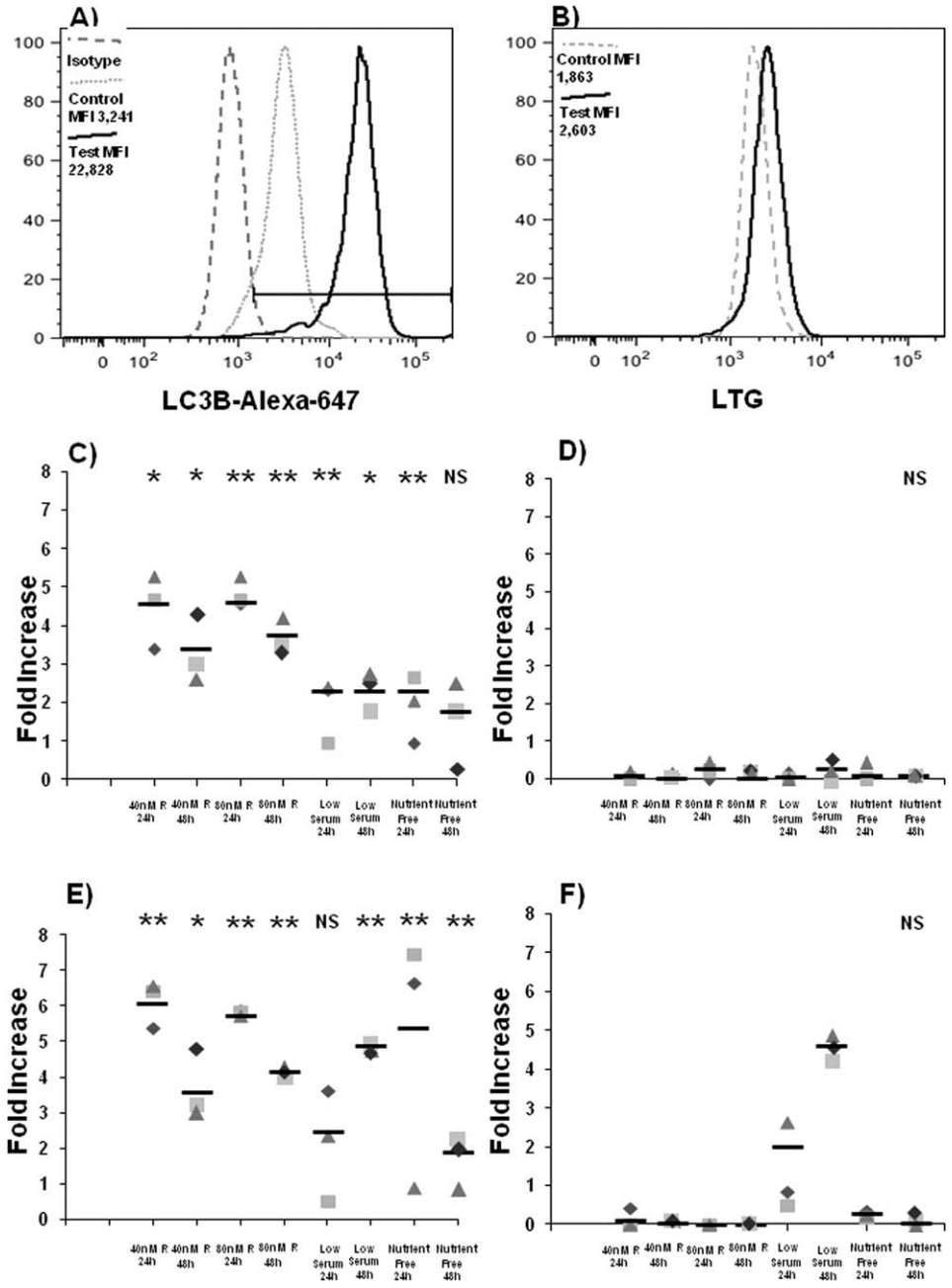

Figure 2. K562 and Jurkat cell lines were untreated or treated with rapamycin at 40 and 80 nM (R), low serum, and nutrient-free growth conditions for 24 and 48 h. Cells were labeled with anti-LC3B-Alexa Fluor647 or isotype-Alexa Fluor647 or 50 nM LTG at 24 and 48 h. Histogram overlays of K562 LC3B expression of isotype control, untreated cells, and cells treated with 80 nM rapamycin at 24 h are shown in (**A**). Histogram overlays of K562 LTG expression of untreated cells and cells treated with 80 nM rapamycin at 24 h are shown in (**B**). Median fluorescence intensity (MFI) values are indicated in (A, B). K562 and Jurkat cell LC3B MFI expressions for untreated or 40 and 80 nM rapamycin, low serum, and nutrient-free growth conditions were determined flow cytometrically at 24 and 48 h and expressed as fold increase above untreated cell controls (**C**, **E**). K562 and Jurkat cell LTG MFI expressions for untreated or 40 and 80 nM rapamycin, low serum, and nutrient-free growth conditions were determined flow cytometrically at 24 and 48 h and expressed as fold increase above untreated cell controls (**D**, **F**). *T* test, $*P = < 0.05$, $**P = < 0.01$; NS, not significant; black bars indicate average fold increase and each individual data point are also shown, $n = 3$.

Discussion

The purpose of this study was to show that flow cytometry can be used to detect the primary autophagy marker, LC3B, when two cell lines are undergoing autophagic flux after treatment with four different inducers of autophagy; these included CQ, rapamycin, serum, and nutrient starvation. LysoTracker dyes also allowed the detection of increased

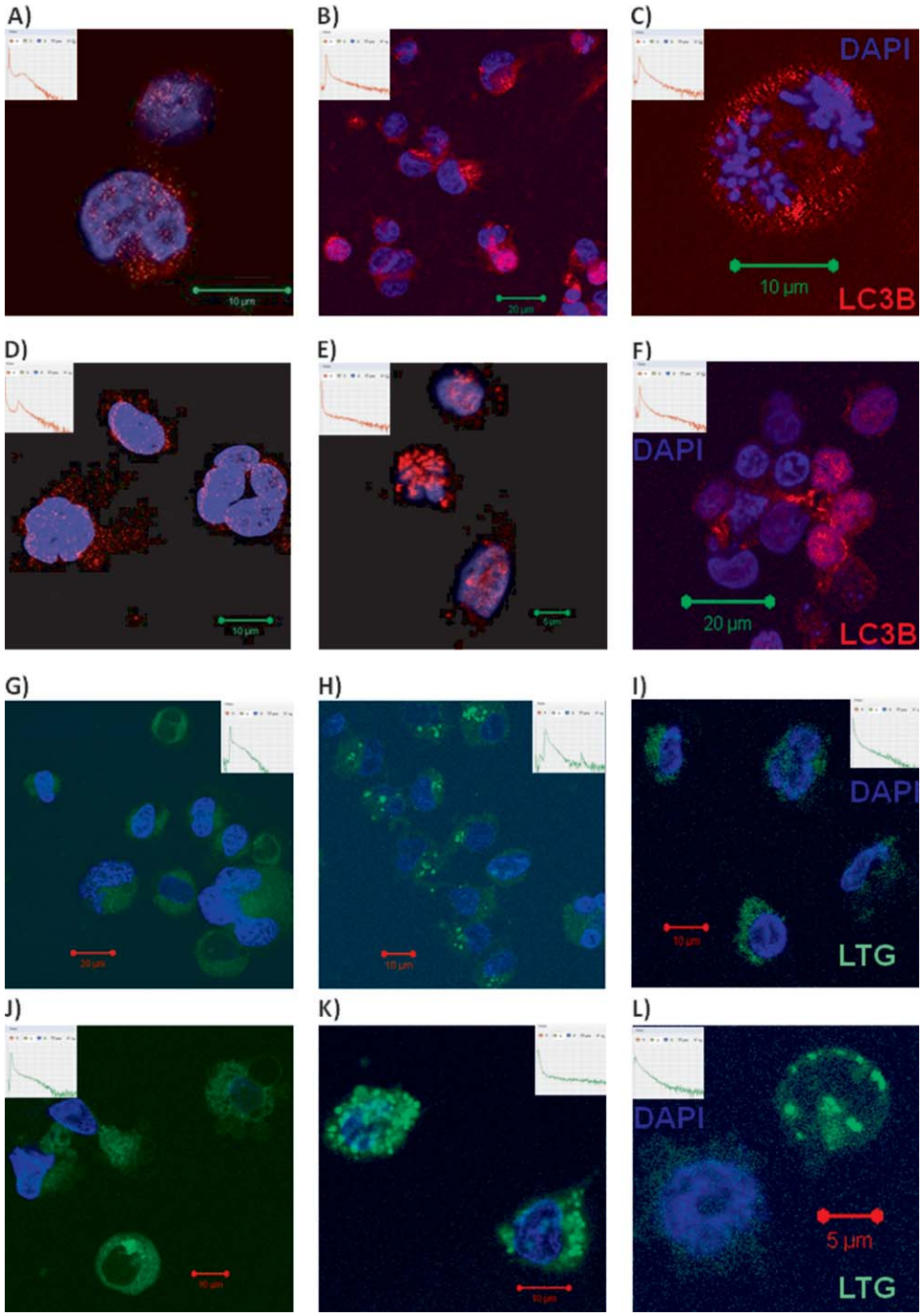

Figure 3. K562 and Jurkat cells untreated (**A**, **D**) or treated with CQ (**B**, **E**) or treated with rapamycin (**C**, **F**) were labeled with anti-LC3B-Alexa-Fluor647, labeled red (or isotype control—data not shown) and counter stained with DAPI (blue) were imaged by confocal microscopy with a 63× objective. K562 and Jurkat cells untreated (**G**, **J**) or treated with CQ (**H**, **K**) or treated with rapamycin (**I**, **L**) were labeled with 50 nM LTG (green) and counter stained with DAPI (blue) were imaged by confocal microscopy with a 63× objective. Fluorescence histograms of 660 and 530 nm emissions from Tiff files were generated and displayed for each image with increasing fluorescence from left to right. Scale bars indicate size.

LTG signal in cells undergoing the autophagic process. The different treatments used show that not only can autophagy be detected when there was a build up of LC3B and LTG signals when cells are not undergoing autophagic flux as in the case of CQ, but also when the cells are undergoing autophagic flux, thus demonstrating the sensitivity of these autophagic flow cytometric assays (26). Although the apparent build up of acidic granules as detected by an increase in LTG signal during the autophagic process this is not a direct measure of autophagy and hence was not expected to match LC3B levels

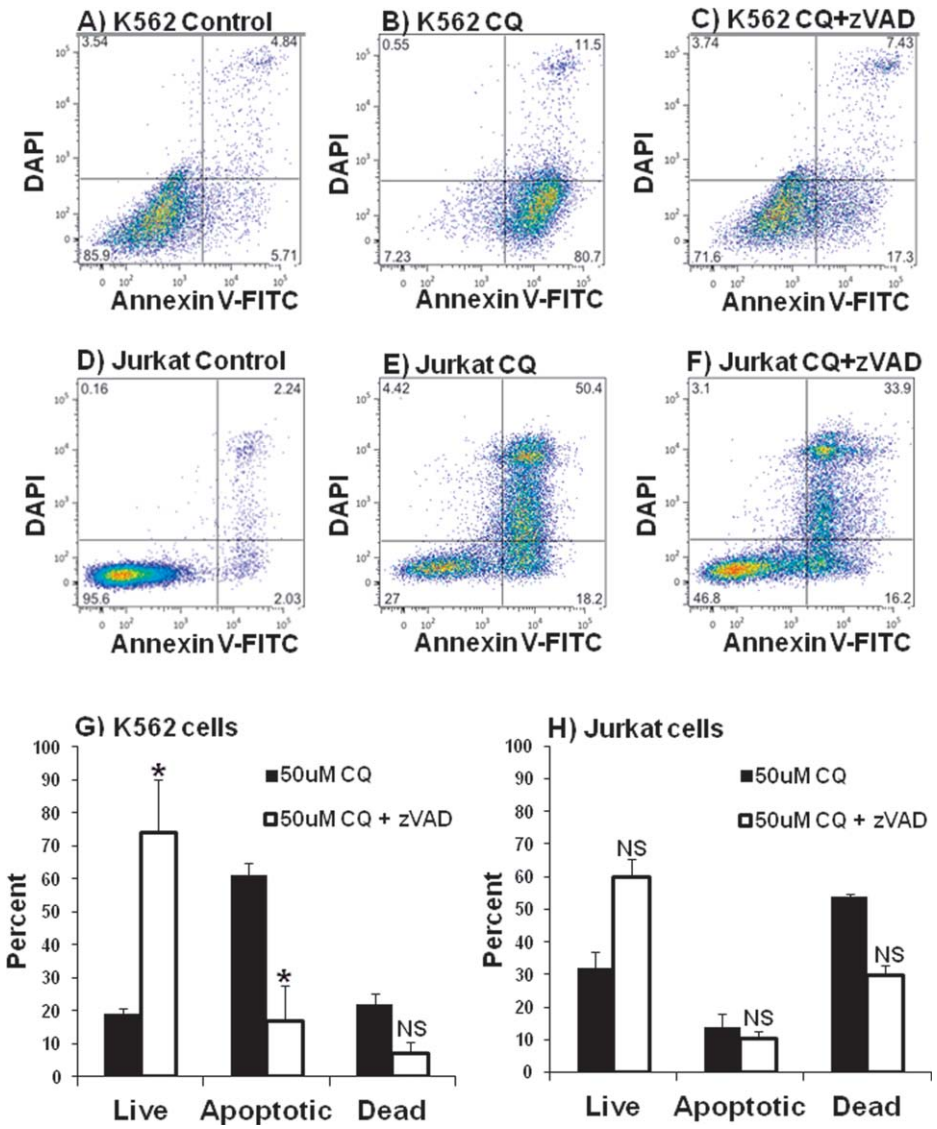

Figure 4. K562 and Jurkat cells were untreated (**A**, **D**) or treated with 50 μM CQ (**B**, **E**) or pretreated for 1 h with pan-caspase blocker, z-VAD (5 μM) before 48-h treatment with 50 μM CQ (**C**, **F**), respectively. K562 and Jurkat cells were labeled with annexin V-FITC and DAPI to determine the level of apoptosis and cell death, $n = 3$ (**G**, **H**), error bars indicate SEM. ANOVA statistical analysis was used to compare differences between CQ treatment and z-VAD with CQ treatment, $*P = <0.05$, $**P = <0.01$, $P = <0.01$; NS, not significant.[Color figure can be viewed in the online issue, which is available at wileyonlinelibrary.com.]

in an identical fashion. However, this study has shown that this LTG upregulation appears biologically to be highly significant as demonstrated by the Phadwal study (26).

The differences due to cell type were apparent with K562 LC3B maximized with 50 μM CQ at 24 h and fell away by 48 h, whilst Jurkat cell LC3B upregulation maximized at 48 h with 50 μM CQ. In contrast, rapamycin induction of autophagy in both cell lines (four to sixfold increase) was similar to LC3B upregulation at 24 and 48 h. Imaging of LC3B in cells treated with CQ and rapamycin showed a general increase above controls as confirmed by fluorescence histogram analysis. Whilst K562 cells undergoing serum and nutrient starvation, although accessing the same signaling route as rapamycin, induced lower LC3B levels. In contrast, Jurkat cells showed a maximum LC3B response with serum and nutrient starvation at 48 and 24 h, respectively. Thus the degree of autophagic responses as demonstrated by LC3B levels varies in different cell types.

LTG upregulation by CQ in Jurkat cells matched LC3B upregulation in terms of time and dose responses. However, K562 cell LTG and LC3B upregulation differed in only the dose of CQ, which maximized at 50 μM for LC3B expression and at 25 μM for LTG. LTG again mirrored the LC3B upregulation induced by rapamycin, which, however, maximized only at 24 h. Imaging of LTG in cells treated with CQ showed a higher increase than that observed for rapamycin above that of controls as confirmed by fluorescence histogram analysis. This difference is probably a reflection of the fact that

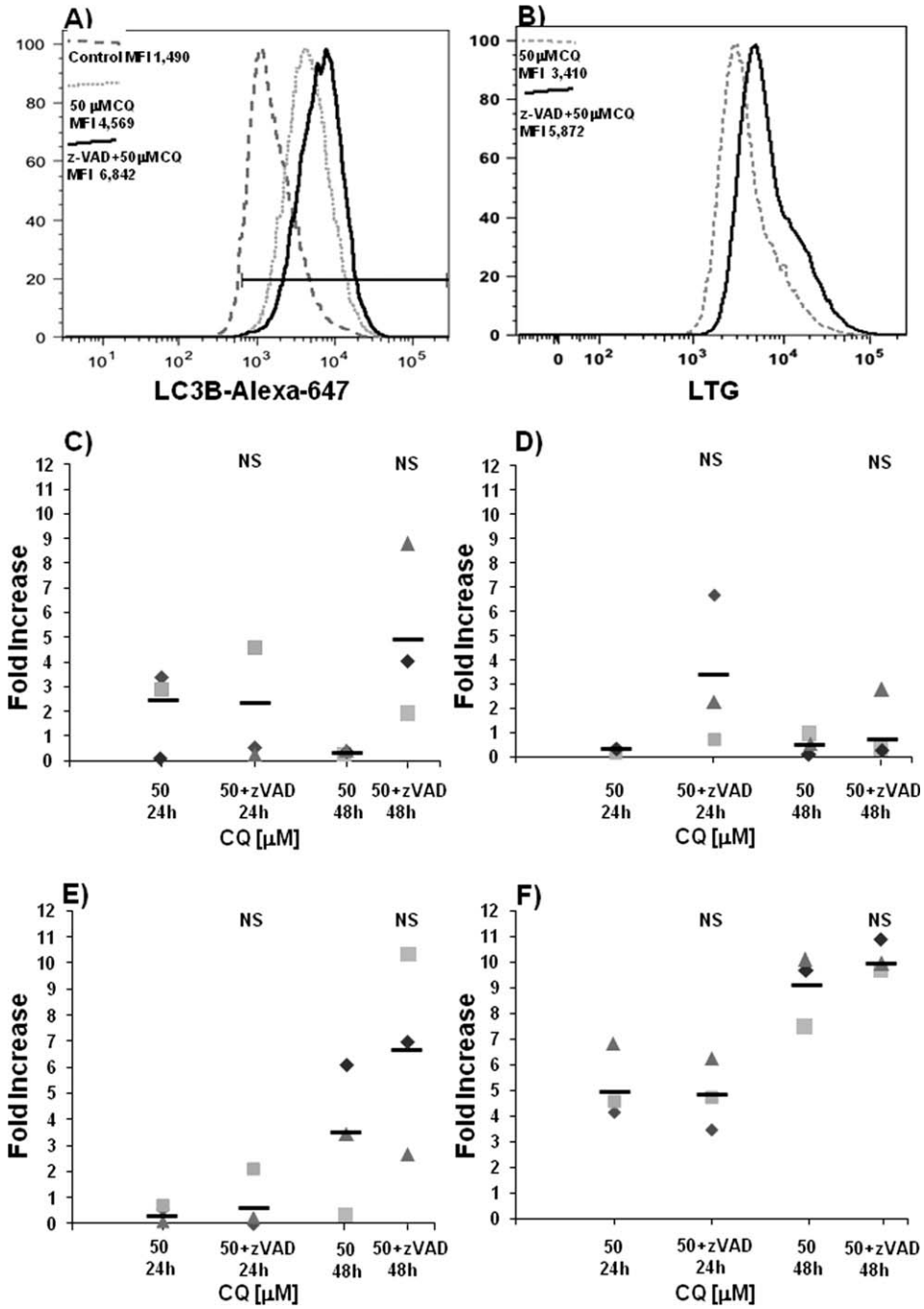

Figure 5. K562 and Jurkat cell lines were untreated or treated with 50 μM CQ or pretreated for 1 h with pan-caspase blocker, z-VAD (5 μM) before 24 and 48-h treatment with 50 μM CQ. Cells were labeled with anti-LC3B-Alexa Fluor647 or isotype-Alexa Fluor647 or 50 nM LTG at 24 and 48 h. Histogram overlays of K562 LC3B expression of untreated cells, cells treated with 50 μM CQ at 48 h, cells treated with z-VAD-50 μM CQ at 48 h are shown in (**A**). Histogram overlays of K562 LTG expression of untreated cells, cells treated with 50 μM CQ at 24 h, or cells treated with z-VAD-50 μM CQ at 24 h are shown in (**B**). Median fluorescence intensity (MFI) values are indicated in (A, B). K562 and Jurkat cell LC3B MFI expressions for untreated cells, cells treated with 50 μM CQ or treated with z-VAD-50 μM CQ were determined flow cytometrically at 24 and 48 h and expressed as fold increase above untreated cell controls (**C**, **E**). K562 and Jurkat cell LTG MFI expressions for untreated cells, cells treated with 50 μM CQ or cells treated with z-VAD-50 μM CQ were determined flow cytometrically at 24 and 48 h and expressed as fold increase above untreated cell controls (**D**, **F**). ANOVA statistical analysis was used to compare differences between CQ treatment and z-VAD with CQ treatment, $*P = <0.5$, $**P = <0.01$; NS, not significant; black bars indicate average fold increase and each individual.

rapamycin-treated cells are undergoing autophagic flux, while CQ treatment blocks this process and hence creates a larger detectable signal. LTG signals during serum starvation of K562 cells showed a minimal (20%) increase at 48 h, whilst Jurkat cells showed this minimal increase during nutrient starvation (10%) and larger responses to serum starvation (two to fourfold increases) at 24 and 48 h, respectively.

Modulation of autophagic marker LC3B and LTG signals would indicate that LTG was measuring autophagy in a commensurate manner to that of LC3B. To this end, as CQ also induces apoptosis, pretreatment with pan-caspase blocker z-VAD would theoretically result in all cells being channeled to autophagy with a resultant upregulation of autophagic marker LC3B and also LTG (30). The effect of z-VAD to block apoptosis was confirmed by employment of the annexin V assay, which showed that cells were rescued from apoptosis. The LC3B signal in K562 and Jurkat cells was shown to be upregulated threefold when treated with z-VAD and CQ at 48 h. This corresponded, in the case of K562 cells, to a similar increase in LTG signal with z-VAD and 50 μM CQ treatment with a threefold increase above that induced by 50 μM CQ treatment alone, but at 24 h (Fig. 5D). In contrast, Jurkat LTG upregulation by z-VAD blocking was not significantly increased at 24 h but increased at 48 h when compared with CQ treatment alone (Fig. 5F).

The use of LC3B antibody staining in flow cytometry has been recently reported and has considerable advantage over their use in microscopy in terms of time (18,26). The employment of LTG dye to measure increased lysosomal mass during autophagy occurs with the upregulation of LC3B (26). In fact, the LCB staining has been shown to co-localize with the lysosome dye Lyso-ID (Enzo Life Sciences) in a proportion of autophagic lymphocytes (26). The LysoTracker dyes are also considerably cheaper per test than the Lyso-ID dye and LC3B antibodies and can be used in cells that are difficult to transfect and are less time consuming in their use than the other methods currently used to study autophagy. This study demonstrates that it is possible to measure autophagic flux flow cytometrically by use of anti-LC3B antibody and LTG labeling of cells. The development of this cheap, reproducible, and easy flow cytometric-based assay to determine the degree of autophagic flux in live cells as well as other cell populations will enhance the ability to study the death processes and mechanisms involved in autophagy in primary cells isolated from patients as well as cell lines.

Acknowledgments

We thank Miss Katy Cogger, BALM Imaging Core Facility, Blizard Institute, for her assistance with confocal microscopy and Dr. Barry Wilbourn, Flow Cytometry Core Facility, Blizard Institute, for his assistance with the preparation of the manuscript.

Literature Cited

1. Ashford TP, Porter K. Cytoplasmic components in hepatic cell lysosomes. J Cell Biol 1962;12:198–202.
2. Deter RL, Duve CD. Influence of glucagon, an inducer of cellular autophagy, on some physical properties of rat liver lysosomes. J Cell Biol 1967;33:437–449.
3. Tooze S, Yoshimori T. The origin of the autophagosomal membrane. Nat Cell Biol 2010;12:12831–12835.
4. Yang Z, Klionsky D. Eaten alive: A history of macroautophagy. Nat Cell Biol 2010;12: 814–822.
5. Shintani T, Klionsky D. Autophagy in health and disease: A double-edged sword. Science 2004;306:990–995.
6. Rosello A, Warnes G, Meier CU. Cell death pathways and autophagy in the central nervous system and its involvement in neurodegeneration, immunity and CNS infection: To die or not to die—That is the question. Clin Exp Immunol 2012;168: 52–57.
7. Xie Z, Klionsky D. Autophagosomes formation: Core machinery and adaptations. Nat Cell Biol 2007;9:1102–1109.
8. Komatsu M, Ichimura Y. MBSJ MCC Young Scientist Award 2009: Selective autophagy regulates various cellular functions. Genes Cell 2010;15:923–933.
9. Hailey DW, Rambold AS, Satpute-Krishnan P, Mitra K, Sougrat R, Kim PK, Lippencott-Schwartz J. Mitochondria supply membranes for autophagosome biogenesis during starvation. Cell 2010;141:656–667.
10. Kim I, Rodriguezenriquez S, Lemasters J. Selective degradation of mitochondria by mitophagy. Arch Biochem Biophys 2007;462:245–253.
11. Mehrpour M, Esclatine A, Beau I, Codogno P. Overview of macroautophagy regulation in mammalian cells. Cell Res 2010;20:748–762.
12. Kabeya Y, Mizushima N, Ueno T, Yamamoto A, Kirisako T, Noda T, Kommani E, Ohsumi Y, Yoshimori T. LC3, a mammalian homologue of yeast Apg8p, is localized in autophagosome membranes after processing. EMBO J 2000;19:5720–5728.
13. Barth S, Glick D, Macleod K. Autophagy: Assays and artifacts. J Pathol 2010;221: 117–124.
14. Hansen TE, Johansen T. Following autophagy step by step. BMC Biol 2011;9:1–4.
15. Shvets E, Fass E, Elazar Z. Utlizing flow cytometry to monitor autophagy in living mammalian cells. Autophagy 2008;4:621–628.
16. Kimura S, Noda T, Yoshimori T. Dissection of the autophagosome maturation process by a novel reporter protein, tandem fluorescent-tagged LC3. Autophagy 2007;3: 452–460.
17. Wu YT, Tan HL, Huang Q, Kim YS, Pan N, Ong WY, Liu ZG, Ong CN, Shen HM. Autophagy plays a protective role during zVAD-induced necrotic cell death. Autophagy 2008;4:457–466.
18. Thomas S, Thurn KT, Biçaku E, Marchion DC, Münster N. Addition of a histone deacetylase inhibitor redirects tamoxifen-treated breast cancer cells into apoptosis, which is opposed by the induction of autophagy. Breast Cancer Res Treatment 2011; 130:437–447.
19. Geng Y, Kohil L, Klocke BJ, Roth KA. Chloroquine-induced autophagic vacuole accumulation and cell death in glioma cells is p53 independent. Neuro-Oncology 2010;12:473–481.
20. Chen Y, McMillan-Ward E, Kong J, Israels SJ, Gibson S. Oxidative stress induces autophagic cell death independent of apoptosis in transformed and cancer cells. Cell Death Differ 2007;15:171–182.
21. Boya P, Gonzalez-Polo RA, Casares N, Perfettini JL, Dessen P, Larochette N, Metivier D, Meley D, Souquere S, Yoshiman T, et al. Inhibition of macroautophagy triggers apoptosis. Mol Cell Biol 2005;25:1025–1040.
22. Boya P, Gonzalez-Polo RA, Poncet D, Andreau K, Vieira HLA, Roumier T, Perfetini JL, Kroemer G. Mitochondrial membrane permeabilization is a critical step of lysosome-initiated apoptosis induced by hydroxychloroquine. Oncogene 2003;22: 3927–3936.
23. Rodriguezenriquez S, Kim I, Currin RT, Lemasters JL. Tracker dyes to probe mitochondrial autophagy (mitophagy) in rat hepatocytes. Autophagy 2006;2:39–47.
24. Byun JY, Yoon CH, An S, Park IC, Kang CM, Kim MJ, Roth KA. The Rac1/MKK7/JNK pathway signals upregulation of Atg5 and subsequent autophagic cell death in response to oncogenic Ras. Carcinogenesis 2009;30:1880–1888.
25. Mellen MA, dela Rosa EJ, Boya P. Autophagy is not universally required for phosphatidyl-serine exposure and apoptotic cell engulfment during neural development. Autophagy 2009;5:964–972.
26. Phadwal K, Alegre-Abarrategui J, Watson AS, Pike L, Anbalagan S, Hammond EM, Wade-Martins R, McMichael A, Klenerman P, Simon AK. A novel method for autophagy detection in primary cells: Impaired levels of macroautophagy in immunosenescent T cells. Autophagy 2012;8:677–689.
27. Shacka JJ, Klocke BJ, Shibata M, Uchiyama Y, Datta G, Schmidt RE, Roth KA. Bafilomycin A1 inhibits chloroquine-induced death of cerebellar granule neurons. Mol Pharmacol 2006;69:1125–1136.
28. Paglin S, Lee NY, Nakar C, Fitzgerlad M, Plotkin J, Deuel B, Hackett AN, McMahill M, Sphicas E, Lampden N, et al. Rapamycin-sensitive pathway regulates mitochondrial membrane potential, autophagy, and survival in irradiated MCF-7 cells. Cancer Res 2005;65:11061–11070.
29. Vega F, Medeiros LJ, Levetaki V, Atwell C, Cho-Vega JH, Tian L, Claret FX, Rassidakiz GZ. Activation of mammalian target of rapamycin signaling pathway contributes to tumor cell survival in anaplastic lymphoma kinase-positive anaplastic large cell lymphoma. Cancer Res 2006;66:6589–6597.
30. Cao C, Subhawong T, Albert JM, Kim KW, Geng L, Sekhar KR, Gi YJ, Lu B. Inhibition of mammalian target of rapamycin or apoptotic pathway induces autophagy and radiosensitizes PTEN null prostate cancer cells. Cancer Res 2006;66:10040–10047.
31. Cho YS, Kwon H. Control of autophagy with small molecules. Arch Pharm Res 2010; 33:1881–1889.